Quasistatic resonance of a chemical potential interruption in a graphene layer and its polarizability: The mixed-polarity semilocalized plasmon

Y. Hadad[*] and Ben Z. Steinberg[†]

School of Electrical Engineering, Tel Aviv University, Ramat-Aviv, Tel-Aviv 69978, Israel
(Received 2 April 2013; revised manuscript received 12 June 2013; published 29 August 2013)

The chemical potential of a graphene layer can be locally interrupted by electrostatic gating or chemical doping. When properly designed, electrically small local interruption can possess quasistatic resonance and be strongly excited by electromagnetic field. This excitation generates a *mixed-type semilocalized* plasmon wave, e.g., it launches TM mode within the interruption domain and TE modes into the surrounding layer. Since the resonance is quasistatic, it is essentially independent of the interruption size and it exists also for sizes much smaller than the corresponding wavelengths of the aforementioned modes. Furthermore, the interruption's polarizability can be defined and calculated. Unlike the conventional polarizability, which is defined directly via a particle's dipole response, here it is defined via the induced currents in the interruption and in its surrounding. We verify our results by comparing them to full-wave numerical simulations. The results have potential applications in many one-atom-thick metamaterials and devices.

I. INTRODUCTION

One-atom-thick metamaterials made of, e.g., graphene layers, have attracted considerable attention. Local electrostatic gating or chemical doping can induce *local interruption* of the chemical potential in an otherwise-perfect infinite graphene layer,[1–5] attaining a "surface inclusion" or a "surface structure" embedded in the graphene background. In Ref. 4 the scattering of graphene plasmons by one-dimensional defects in the chemical potential was studied via an integral equation procedure. Dispersion of surface plasmons propagating on a graphene layer with a one-dimensional conductivity modulation was studied in Ref. 5. In Refs. 6 and 7 it has been shown that the extreme case of a single-point defect in a graphene layer may constitute an atomic surface plasmon resonator of subnanometer scale. In Ref. 8 the polarizability of *disjoint* graphene nanodisks was used to study the absorption by an array of graphene patches. It should be emphasized that in these previous studies, patch or interruption *resonance* is based on interference of internal waves; hence it is size dependent and not quasistatic.

Modeling multiscale problems, e.g., the design of metamaterials and structures made of a large number of subwavelength inclusions, can be efficiently addressed using polarizability theory. The excitation of a subwavelength particle exposed to a local exciting field E_0^L (the local field in the absence of the particle) can be modeled as a dipolar moment p. The particle's internal dynamics is entirely encapsulated in its polarizability α, defined via the relation $p = \alpha E_0^L$. Interparticle interactions are taken into account via the medium's Green function. The electric response of deep subwavelength metallic particles, the associated quasistatic resonance, and the polarizability were studied in a number of publications (see, e.g., Ref. 9). The technique has been used for the study of one-dimensional plasmonic particle chains,[10–14] as well as for the study of metasurfaces that consist of two-dimensional arrays of resonating particles.[15–19]

Here we study the excitation physics and the polarizability of an electrically small circular interruption of radius R in an otherwise-perfect infinite graphene layer as shown in Fig. 1. Since graphene layers can be modeled by local conductivities

down to nanometer scales,[20] the latter and the former are characterized by their surface conductivities $\sigma_{1,2}$, respectively, as obtained from the Kubo formula.[21] We show that it may exhibit a quasistatic resonance that is independent of R, and takes place when $\Im\{\sigma_1 + \sigma_2\} = 0$. Due to the opposite signs of the $\sigma_{1,2}$ imaginary parts, this resonance possesses a unique structure of a *semilocalized mixed-modes plasmon*; e.g., when $\Im\{\sigma_{1,2}\} \lessgtr 0$ the interruption itself (σ_2) is of inductive nature, supporting a TM mode with current confined essentially to the interruption area, but also "spills over" to the surrounding graphene layer (σ_1) that is of capacitive nature and supports a TE mode. See Fig. 1(b) for an example of the currents that spills out to the graphene layer. The mixed polarity nature of the excitation is shown in Fig. 2. We study this resonance and also extend the concept of polarizability to this important class of problems. If one can use polarizability to model the response of a single interruption, interinterruption dynamics in a system of many interruptions can be studied using the Green function of a homogeneous medium in the presence of a graphene sheet.[22,23] Note, however, that the following issues naturally arise:

1. While the electric charge and current occupy the *entire* plane, the interruption's dipole moment p and the ensuing polarizability α are supposed to replace *only* the interruption itself, and not the current and charge that are "all over" the plane.

2. What, then, is the extent or component of the current/charge that should be included in the evaluation of p and α? And what should be left out?

3. The component of the current/charge that is not included in the evaluation of p should be considered as a *result* of the existence of p; i.e., it is *driven* by it. Hence, the current that is included in the evaluation of p should be considered as a *source*. What is the formulation that makes this distinction *unique*?

4. To address these issues we provide below an equivalent formulation and obtain an ensuing equivalent current k_e that exists on an infinite homogeneous graphene layer. k_e is *not* the actual current k. The relation between them is given below.
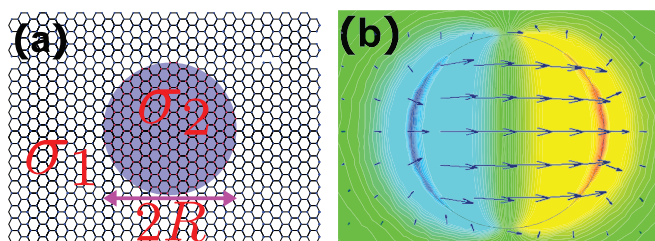
FIG. 1. (Color online) (a) A circular interruption in a graphene layer. (b) The normal field E_z (color map) and current (arrows) responses to $\boldsymbol{E}_0 = \hat{\boldsymbol{x}} E_0$ for $R = 3$ nm and parameters as in the numerical example below, calculated by CST STUDIO at $f = 62.7$ THz. E_z ranges between ± 1.44 kv/m (red and blue colors). The surface charge is given by $\eta = 2\epsilon_0 E_z$. The current spills out of the interruption domain, creating a semilocalized plasmon excitation.

Despite this fact, $\boldsymbol{k}_e$ provides the interruption's equivalent dipole, as seen in our analysis and verified by full-wave simulations.

The points raised above should be contrasted with conventional cases of quasistatically resonating *disjoint* plasmonic particles studied in Refs. 9–19, where the current and charge are confined within the particle's volume. It should also be contrasted with Ref. 8 that deals with large, nonquasistatic, and yet *disjoint* graphene disks. Thus we derive α via the surface currents excited on the entire graphene layer by using our specially tailored equivalent problem. Our result can then be used in the design of electrically tuned one-atom-thick metasurfaces, IR optical components, defects analysis, etc. Moreover, the procedure presented here can also be applied for an *ab initio* calculation of α of few atoms defects as in Refs. 6 and 7.

II. FORMULATION

We define the problem as follows. Consider an infinite graphene layer on a $z = 0$ plane, exposed to a localized circular
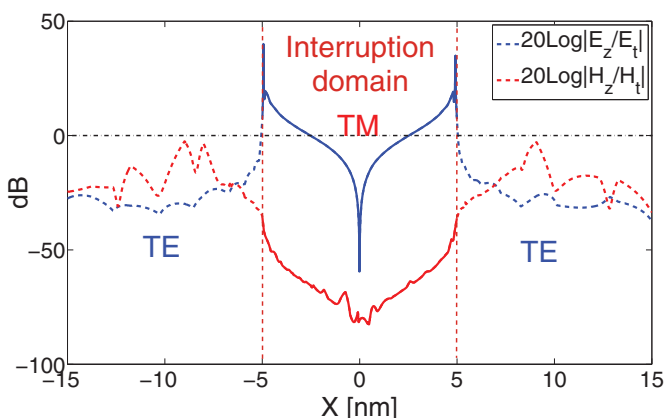

FIG. 2. (Color online) The relation between the normal and transverse fields as obtained from full-wave numerical simulations by CST STUDIO, along the line $y = 0$ for an interruption with $R = 5$ nm with parameters as in the numerical examples below, and at resonance. The mixed-polarity property (TM inside, TE outside) is evident. Essentially similar results are obtained along other lines and for smaller values of R.

spot of a *static* electric field on a subwavelength domain with radius R. The chemical potential would be locally interrupted, leading to the surface conductivity of σ_2 (σ_1) for $\rho < R$ ($\rho > R$) according to the Kubo formula.[21] The system and a typical charge response are shown in Fig. 1. We define $[(\boldsymbol{E}_0, \boldsymbol{H}_0)] (\boldsymbol{E}, \boldsymbol{H})$ as the total [un]interrupted fields excited by a time harmonic source in the [absence] presence of the interruption. Our goal is to study the interruption response in terms of the excited currents and to qualify the interruption by some polarizability α such that the total field in the interrupted case, outside of the interruption domain, would be $(\boldsymbol{E}_0, \boldsymbol{H}_0)$ plus the fields of a dipole with moment $\boldsymbol{p} = \alpha \boldsymbol{E}_0$.

We start by solving for the surface current, which forms the basis for deriving the dipole moment and the polarizability. Since the latter is nothing but the interruption's equivalent representation, a rigorous mathematical definition of the equivalent problem is in order. The uninterrupted fields obey

$$\nabla \times \boldsymbol{E}_0 = i\omega\mu \boldsymbol{H}_0, \tag{1a}$$

$$\nabla \times \boldsymbol{H}_0 = -i\omega\epsilon \boldsymbol{E}_0 + \delta(z)\sigma_1 \boldsymbol{E}_0^t, \tag{1b}$$

where the superscript t denotes the field's tangential component. The fields in the presence of the interruption obey

$$\nabla \times \boldsymbol{E} = i\omega\mu \boldsymbol{H}, \tag{2a}$$

$$\nabla \times \boldsymbol{H} = -i\omega\epsilon \boldsymbol{E} + \delta(z) \begin{cases} \sigma_2 \boldsymbol{E}^t & \rho < R \\ \sigma_1 \boldsymbol{E}^t & \rho > R. \end{cases} \tag{2b}$$

We define the equivalent mathematical problem by introducing a localized field-dependent surface current $\boldsymbol{k}_e$ such that the governing formulation possesses the same structure as that of Eq. (1a), plus the localized term that lies on an *uninterrupted* layer with σ_1. Hence our equivalent formulation is

$$\nabla \times \boldsymbol{E} = i\omega\mu \boldsymbol{H}, \tag{3a}$$

$$\nabla \times \boldsymbol{H} = -i\omega\epsilon \boldsymbol{E} + \delta(z)\sigma_1 \boldsymbol{E}^t + \delta(z)\boldsymbol{k}_e, \tag{3b}$$

where

$$\boldsymbol{k}_e = \begin{cases} (\sigma_2 - \sigma_1)\boldsymbol{E}^t & \rho < R \\ 0 & \rho > R. \end{cases} \tag{4}$$

$\boldsymbol{k}_e$ can be viewed as a source, and it compensates for the presence of σ_2. The scattered fields $\boldsymbol{E}_s = \boldsymbol{E} - \boldsymbol{E}_0$ and $\boldsymbol{H}_s = \boldsymbol{H} - \boldsymbol{H}_0$ can be shown to obey exactly the same formulation of Eqs. (3a)–(4). Furthermore, by comparing this formulation for the scattered fields to Eq. (1a), we conclude that $\boldsymbol{k}_e$ is the relevant current component that determines the dipole moment associated with the interruption. Now, in order to "close the loop" we need to relate $\boldsymbol{k}_e$ to the *uninterrupted* field $\boldsymbol{E}_0$. Once this linear relation $\boldsymbol{k}_e(\boldsymbol{E}_0)$ is known, the interruption's equivalent dipole moment $\boldsymbol{p}$ and its polarizability α are obtained from

$$\boldsymbol{p} = \frac{i}{\omega} \int_{S_{\text{int}}} \boldsymbol{k}_e(\boldsymbol{E}_0) dS = \alpha \boldsymbol{E}_0, \tag{5}$$

where S_{int} is the interruption's area. A few important points should be emphasized. First, despite the fact that $\boldsymbol{k}_e$ is the quantity that determines the dipole excitation, it is *not* the true physical current within the interruption area. The latter and the

former are related via

$$k_e = \frac{\sigma_2 - \sigma_1}{\sigma_2} k(r), \quad \rho < R \tag{6}$$

and $k_e = 0$ for $\rho > R$. Second, note that this is a *quasistatic* problem, since we assume that the interruption size is electrically small ($R \ll \lambda$) with respect to the wavelength of *all possible* wave spectra in the problem. (The shortest wavelength in the examples below corresponds to the TM mode of the graphene layer.) Finally, we note that once the relation in Eq. (5) is derived, the fields at observation points located sufficiently far from the interruption (say, $r > 2.5R$) and either on or off the layer, can be described by the dyadic Green's function above homogeneous graphene,[22] weighted by p.

We now derive the quasistatic solution for the actual current $k(\rho)$, from which k_e and p are obtained via Eqs. (5) and (6). Clearly, for an uninterrupted layer exposed to a static and uniform electric field $\boldsymbol{E}_0 = E_0 \hat{\boldsymbol{x}}$, one obtains a flow of a static surface current $\boldsymbol{k}_0 = k_0 \hat{\boldsymbol{x}} = \sigma_1 E_0 \hat{\boldsymbol{x}}$. In the presence of the interruption, and under quasistatic excitation, we express the total surface current as $\boldsymbol{k} \cong \boldsymbol{k}^{(0)} + \boldsymbol{k}^{(1)}$, where the zero-order term $\boldsymbol{k}^{(0)}$ is a solution of a static problem and $\boldsymbol{k}^{(1)}$ is a quasistatic correction approximated via the time derivative of surface charge density of the zero-order solution. As we shall see below, $\boldsymbol{k}^{(1)}$ may not be negligible in the domain of parameters of interest. In the following we begin with $\boldsymbol{k}^{(0)}$.

In statics $\nabla \times \boldsymbol{E} = 0$, which leads to $\nabla_t \times \boldsymbol{E}^t = 0$, where ∇_t is the transverse part of ∇. In addition, $\boldsymbol{k}(\rho) = \sigma \boldsymbol{E}^t(\rho)$, where σ is a piecewise constant function of ρ and $\boldsymbol{\rho} = (\rho, \phi)$ is the polar coordinate on the $2D$ sheet. Hence a potential can be defined by $\boldsymbol{E}^t(\rho) = -\nabla_t \Phi(\rho)$. Moreover, charge conservation requires $\nabla_t \cdot \boldsymbol{k}(\rho) = 0$ and hence $\nabla_t^2 \Phi_{1,2}(\rho) = 0$ in the two conductivity regions 1 and 2. Under the excitation $\boldsymbol{E}_0 = E_0 \hat{\boldsymbol{x}}$ the potentials $\Phi_{1,2}(\rho)$ are subject to the following conditions:

(1) $\Phi_1(\rho \to \infty) = -E_0 \rho \cos \phi$.
(2) $\Phi_2(\rho = 0)$ is regular.
(3) $\Phi_1 = \Phi_2|_{\rho=R}$.
(4) $\sigma_1 \partial_\rho \Phi_1 = \sigma_2 \partial_\rho \Phi_2|_{\rho=R}$.

The potential solution is given by the sum of primary and secondary potentials $\Phi_{1,2} = \Phi^p + \Phi_{1,2}^s$, where $\Phi^p = -E_0 \rho \cos \phi$ (representing the uninterrupted solution), and

$$\Phi_1^s(\rho) = A \frac{R^2}{\rho} \cos \phi, \quad \Phi_2^s(\rho) = A \rho \cos \phi, \tag{7}$$

where

$$A = \frac{\sigma_2 - \sigma_1}{\sigma_2 + \sigma_1} E_0. \tag{8}$$

Using Eqs. (6)–(8) and the conditions above, we calculate the zero-order surface current distribution inside the interruption domain:

$$\boldsymbol{k}^{(0)} = \frac{2\sigma_1 \sigma_2}{\sigma_2 + \sigma_1} E_0 \hat{\boldsymbol{x}}, \quad \rho < R. \tag{9}$$

The current outside can be calculated as well, but it will not be needed in the following derivations. From Eqs. (7)–(9) it becomes clear that $\boldsymbol{k}^{(0)}(\rho)$ resonates had $\Im\{\sigma_1 + \sigma_2\} = 0$ inside as well as outside the interruption domain. A surface charge is accumulated in the interruption's vicinity. It will be calculated next and used to find $\boldsymbol{k}^{(1)}$. Consider now the potential

outside the surface ($z \neq 0$), governed by the Laplace equation. Moreover, at $z = 0$ it must obey continuity with the potential in Eqs. (7) and (8). One may readily verify that the following superposition of the cylindrical harmonics $\cos(\phi) J_1(\kappa \rho) e^{-\kappa |z|}$,

$$\Phi^s(\boldsymbol{r}) = \cos \phi \int_0^\infty d\kappa \, \kappa \, J_1(\kappa \rho) e^{-\kappa |z|} F(\kappa), \tag{10}$$

satisfies the Laplace equation in the two half-spaces $z > 0$ and $z < 0$ separately, and vanishes as $|z| \to \infty$. $F(\kappa)$ can be obtained by imposing continuity between $\Phi^s(\boldsymbol{r})$ and the on-sheet potentials in Eq. (7), and by using the Bessel-transform pair. Calculation yields

$$F(\kappa) = A \frac{2R}{\kappa^2} J_1(\kappa R). \tag{11}$$

Next, by employing the boundary condition for the normal fields on $z = 0$ one may obtain the surface charge density accumulated on the surface impedance sheet,

$$\eta^{(0)}(\rho) = 4R\epsilon_0 A \cos \phi \int_0^\infty d\kappa \, J_1(\kappa \rho) J_1(\kappa R). \tag{12}$$

Next, we relate $\boldsymbol{k}^{(1)}$ to $\eta^{(0)}$ via charge conservation $\nabla_t \cdot \boldsymbol{k}^{(1)} = i\omega \eta^{(0)}$. Using Eq. (12) one obtains

$$\nabla_t \cdot \boldsymbol{k}^{(1)} = B \cos(\phi) f(u), \tag{13a}$$

where $u = \rho/R$ and

$$B = 4i\omega \epsilon_0 A, \quad f(u) = \int_0^\infty J_1(su) J_1(s) ds. \tag{13b}$$

An *exact* solution to Eq. (13a) is, e.g.,

$$\boldsymbol{k}^{(1)} = \hat{\boldsymbol{x}} R B g(u), \quad \text{with} \quad g'(u) = f(u), \tag{14}$$

that as with $\boldsymbol{k}^{(0)}$ in Eq. (9), resonates having $\Im\{\sigma_1 + \sigma_2\} = 0$, but needs an integration constant for it to be unique. Note that the condition $\lim_{u\to\infty} \boldsymbol{k}^{(1)} = 0$, which makes sense physically, may not yield the correct result since $\boldsymbol{k}^{(1)}$ is a quasistatic correction that is not valid far from the interruption domain. However, in light of Eqs. (5) and (6) for α, we only need the surface integral of $\boldsymbol{k}^{(1)}$ over the interruption area; the specific shape of $g(u)$ is unimportant. We have

$$\int_{\rho<R} \boldsymbol{k}^{(1)} dS = \hat{\boldsymbol{x}} 2\pi R^3 B \int_0^1 u g(u) du = \hat{\boldsymbol{x}} B R^3 C. \tag{15}$$

Furthermore, note that $f(u)$ and $g(u)$ are dimensionless functions independent of any physical parameter of the problem. All the electrical parameters are in B. Hence $C = 2\pi \int_0^1 u g(u) du$ is a *universal constant* that can be obtained by a single one-parameter fitting to a full-wave numerical solution. Following this procedure we obtained $C = \pi/8$. We emphasize that this constant does not depend on any of the problem parameters but only on the fact that the interruption size is sufficiently small so that the first-order quasistatic solution is valid.

Since $\boldsymbol{k} \approx \boldsymbol{k}^{(0)} + \boldsymbol{k}^{(1)}$, we may use now Eqs. (15) and (9) in Eqs. (5) and (6) to obtain α. The result is

$$\alpha = \frac{\pi R^2}{-i\omega} \left[2\sigma_1 \sigma_2 + \frac{i}{2} \frac{k_0 R}{\eta_0} (\sigma_2 - \sigma_1) \right] \frac{1}{\sigma_2} \frac{\sigma_2 - \sigma_1}{\sigma_1 + \sigma_2}. \tag{16}$$
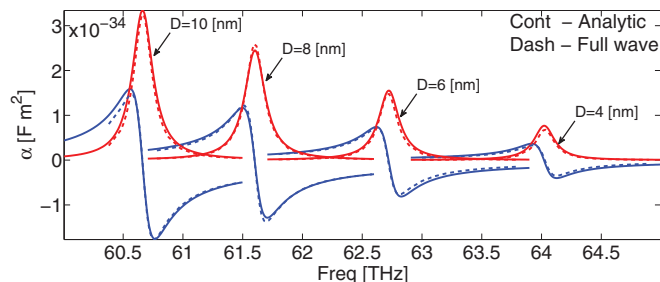
FIG. 3. (Color online) Analytical and numerical results for α as a function of frequency: blue- $\Re\{\alpha\}$, red- $\Im\{\alpha\}$.

Note that α possesses resonance when $\Im\{\sigma_1 + \sigma_2\} = 0$. By virtue of the quasistatic correction, Eq. (16) incorporates approximately the interruption's radiation loss and other mechanisms such as the graphene layer absorption.

III. EXAMPLES

We turn now to compare our analytic results to a full-wave solutions carried out by CST STUDIO.[24] We calculate α for several values of R, temperature $T = 3$ K, chemical potentials $\mu_{c_1} = 0.15$ eV and $\mu_{c_2} = 0.2$ eV, and damping factor $\Gamma = 2.7$ meV. In Fig. 3 α is compared to full-wave simulations. The resonance condition $\Im\{\sigma_1 + \sigma_2\} = 0$ is at $f = 67.29$ THz, however, due to finite interruption size. A resonance redshift ranging between 5% for the smaller interruption to 10% for the largest one was observed and compensated in the figure (i.e., the analytic results were shifted leftwards by the corresponding resonance mismatch). The polarizability is depicted as a function of the frequency with R being a parameter. Note the good matching of the resonance linewidths.

With these simulation parameters the background layer and the interruption conductivities near resonance are $\sigma_{1,2} \approx \mp i2.1 \times 10^{-5} + 4.5 \times 10^{-7}$. [Siemens] σ_2 supports a TM mode that is highly confined and with a relatively short wavelength (≈ 22 nm), compared with the surrounding layer σ_1 that supports a weakly confined TE mode with an approximate wavelength of vacuum (≈ 4200 nm). With these parameters, the ratio between the static and quasistatic terms of α is about 1:0.5 (1:0.2) for the interruption of $D = 10$ nm ($D = 4$ nm). Therefore, as anticipated above, the quasistatic correction cannot be ignored. We observe that the quasistatic resonance condition extensively used in the context of local plasmons in noble metals can also be used in graphene plasmonics to design remarkably localized resonators. Next, we examine the validity of the equivalent problem presented in Eqs. (1a)–(4) for the definition of a disjoint dipole on a homogeneous graphene
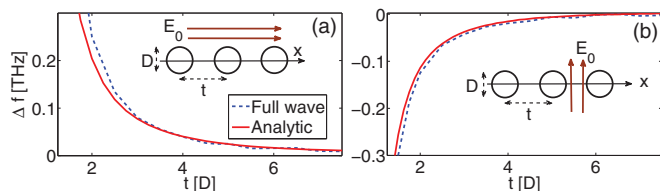

FIG. 4. (Color online) (a) The exciting field is parallel to the particle axis, a resonance redshift is observed. (b) The exciting field is normal to the particles axis, a resonance blueshift is observed.
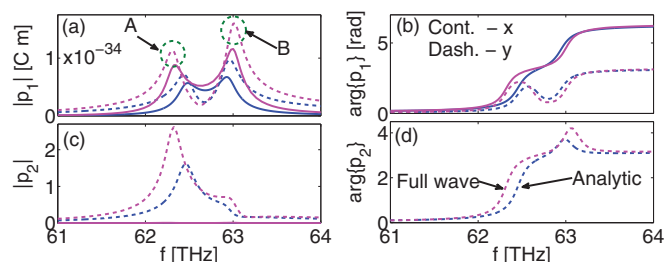

FIG. 5. (Color online) (a,c) Magnitude and (b,d) phase of the x and y components (cont. and dashed, respectively) of the dipoles ($p_{1,2}$) of the triangular configuration shown in Fig. 6. p_3 is essentially the same as p_1, but with π added to the phase of $p_{3,y}$. Blue lines: analytic, magenta: full-wave solution.

layer. To that end, we calculate the resonance frequency shift due to the coupling between three adjacent interruptions via the dyadic Green's function $\mathbf{G}(\boldsymbol{r}, \boldsymbol{r}')$ on an infinite graphene sheet.[22] Using the polarizability approach, a system of N interruptions is governed by the matrix equation

$$\alpha_m^{-1} \boldsymbol{p}_m = \sum_{n, n \neq m}^N \mathbf{G}(\boldsymbol{r}_m, \boldsymbol{r}_n) \boldsymbol{p}_n + \boldsymbol{E}_0(\boldsymbol{r}_m), \qquad (17)$$

with $m = 1, \ldots N$, and where $\alpha_n, \boldsymbol{r}_n, \boldsymbol{p}_n$ are the nth interruption's polarizability, center location, and dipole response, respectively. A comparison between the polarizability-based analytic formulation in Eqs. (16) and (17) and full-wave results is shown in Figs. 4(a) and 4(b). In Fig. 3(a)[b] the excitation field is parallel [normal] to the particles coaxis. In this case the resonance frequency is lower [higher] than the resonance frequency of a single interruption. The analytic result becomes valid when the spacing between the particles is larger than $t \approx 3D$ [$t \approx 2D$]. In addition, note that large frequency shift indicates strong coupling between the interruptions. Moreover, it may be noticed that for a given interparticle spacing t the frequency shift in the parallel case [Fig. 3(a)] is larger than that in the transverse case [Fig. 3(b)]. Hence we conclude that the interparticle interactions in the longitudinal case are stronger—in accord with known results for particle chains in homogeneous medium.[13]

In Figs. 5 and 6 we compare the excitation amplitudes and phases of three interruptions located on the three vertexes of an equal-sides triangle due to a $\hat{\boldsymbol{y}}$-polarized plane wave that hits the graphene layer. The spacing between the interruptions is $t = 1.5D$. This small distance is chosen in order to
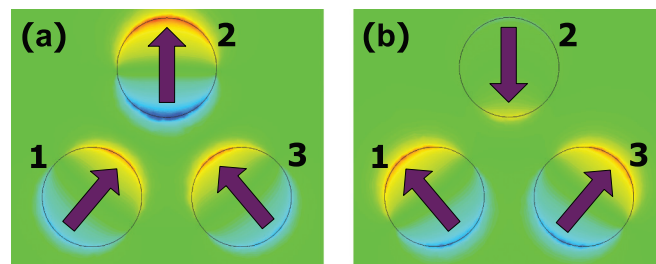

FIG. 6. (Color online) Charge distribution for the triangle configuration as obtained by CST: (a) lower resonance [Fig. 5(a) point A] and (b) upper resonance [Fig. 5(a), point B].

enhance the coupling effects. Although it is smaller than the $2 - 3D$ distance required for accurate results, the physics is clearly revealed and with no qualitative differences in the response. In Fig. 5 the magnitude and phase of the x and y components (cont. and dashed, respectively) of each dipole are shown. The blue lines present the excited dipoles as obtained from the analytic results, whereas the magenta lines present an approximation for the excited dipoles obtained via sampling of the full-wave simulation current in the center of each interruption and by the assumption that it is uniform on the entire interruption domain. The exciting field is y polarized. Due to symmetry, two modes can be excited and observed. The lower [upper] resonance, marked by a green circle at point A [B] in Fig. 5(a) is a "bonding," or inphase-like ["anti-bonding" or antiphase-like] mode. A picture of its dipoles is shown in Fig. 6(a)[b]. Note that Fig. 6 only shows a "snapshot" of the system; the dipoles actually oscillate in time. Also, the antiphase-like mode seems to be associated with higher electromagnetic energy. This energy is provided by the time-harmonic source (plane wave) that excites the system.

IV. CONCLUSIONS

We have shown that an electrically small chemical potential interruption in a graphene layer may possess a quasistatic resonance that launches a *mixed-type semilocalized* plasmon wave: a TM mode within the interruption domain, and TE modes into the surrounding layer. By using an equivalent problem formulation, we have derived the interruption's polarizability which enables one to interpret the interruption itself as an equivalent source that is proportional to the local tangential field, launching currents over the entire graphene layer. In analogy to particles plasmonics, our polarizability can be used to study the electrodynamics of one-atom-thick metasurfaces made of a system of interruptions in an otherwise-perfect graphene layer.

ACKNOWLEDGMENT

*hadady@eng.tau.ac.il

†Corresponding author: steinber@eng.tau.ac.il

[1] A. Vakil, N. Engheta, Science **332**, 1291 (2011).

[2] S. Thongrattanasiri, I. Silveiro, and F. J. Garcia de Abajo, Appl. Phys. Lett. **100**, 201105 (2012).

[3] E. Forati and G. W. Hanson, arXiv:1306.3143v2.

[4] J. L. Garcia-Pomar, A. Y. Nikitin, and L. Martin-Moreno, ACS Nano **7**, 4988 (2013).

[5] N. M. R. Peres, A. Ferreira, Y. V. Bludov, and M. I. Vasilevskiy, J. Phys.: Condens. Matter **24**, 245303 (2012).

[6] W. Zhou, J. Lee, J. Nanda, S. T. Pantelides, S. J. Pennycook, and J. C. Idrobo, Nat. Nanotechnol. **7**, 161 (2012).

[7] W. Zhou, M. D. Kapetanakis, M. P. Prange, S. T. Pantelides, S. J. Pennycook, and J. C. Idrobo, Phys. Rev. Lett. **109**, 206803 (2012).

[8] S. Thongrattanasiri, F. H. L. Koppens, and F. J. Garcia de Abajo, Phys. Rev. Lett. **108**, 047401 (2012).

[9] F. Wang and Y. R. Shen, Phys. Rev. Lett. **97**, 206806 (2006).

[10] M. Quinten, A. Leitner, J. R. Krenn, and F. R. Aussenegg, Opt. Lett. **23**, 1331 (1998).

[11] M. L. Brongersma, J. W. Hartman, and H. A. Atwater, Phys. Rev. B **62**, R16356 (2000).

[12] S. A. Tretyakov and A. J. Viitanen, Electrical Engineering **82**, 353 (2000).

[13] A. Alu and N. Engheta, Phys. Rev. B **74**, 205436 (2006).

[14] D. V. Orden, Y. Fainman, and V. Lomakin, Opt. Lett. **34**, 422 (2009).

[15] W. Gotschy, K. Vonmetz, A. Leitner, and F. R. Aussenegg, Opt. Lett. **21**, 1099 (1996).

[16] W. Gotschy, K. Vonmetz, A. Leitner, and F. R. Aussenegg, Appl. Phys. B **63**, 381 (1996).

[17] K. E. Jordan, G. R. Richter, and P. Sheng, J. Comput. Phys. **63**, 222 (1986).

[18] S. Steshenko, F. Capolino, P. Alitalo, and S. Tretyakov, Phys. Rev. E **84**, 016607 (2011).

[19] A. L. Fructos, S. Campione, F. Capolino, and F. Mesa, JOSA B **28**, 1446 (2011).

[20] S. Thongrattanasiri, A. Manjavacas, and F. J. Garcia de Abajo, ACS Nano **6**, 1766 (2012).

[21] V. P. Gusynin, S. G. Sharapov, and J. P. Carbotte, J. Phys.: Condens. Matter **19**, 026222 (2007).

[22] George W. Hanson, J. Appl. Phys. **103**, 064302 (2008).

[23] George W. Hanson, A. B. Yakovlev, and A. Mafi, J. Appl. Phys. **110**, 114305 (2011).

[24] CST STUDIO SUITE, 2012; www.cst.com